International Journal of Control, Automation and Systems 18(10) (2020) 2456-2467
http://dx.doi.org/10.1007/s12555-019-0343-7
ISSN:1598-6446 eISSN:2005-4092
http://www.springer.com/12555

PID Principles to Obtain Adaptive Variable Gains for a Bi-order Sliding Mode Control

Sergio Alvarez-Rodríguez* and Gerardo Flores

Abstract: A new model to obtain adaptive variable gains for a bi-order Sliding Mode Control is proposed in this work. The variable gains for the controller are designed to dynamically adapt their values, using principles of the well-known Proportional-Integral-Derivative control technique, where the magnitude of the tracking error is the signal feedback. According to the way to tune parameters, it can become a first-order or a second-order controller. This design takes into account the actuators' constraints (operational limits of the plant to control). As a result of the adaptive properties of the proposed scheme, the new controller significantly reduces the energy consumption in control processes, and it rejects the so-called chattering-effect, simultaneously maintaining the main robust properties of the Sliding Mode strategy. In order to show the feasibility and effectiveness of the proposed design, simulation results are presented, where the performance of the proposed controller is compared with the conventional Sliding Modes of order one and two, and also with the classical PID controller. A strong stability analysis in the sense of Lyapunov is presented, showing global exponential stability for the equilibrium point of the closed-loop control system when the proposed control design is used.

Keywords: Chattering-effect, Lyapunov stability approach, PID control, sliding mode control.

1. INTRODUCTION

Sliding Mode Control (SMC) is used to design robust controllers for a large variety of nonlinear systems (see [1]). SMC strategy uses a discontinuous control law to drive the system state from an arbitrary initial state to the origin along a previously specified trajectory, i.e., the sliding manifold [2]. The main advantages of Sliding Modes (SM) are robustness to parameter uncertainty and invariance to unknown disturbances [3]. However, as it is stated by [4–6] (among others), SMC has a major drawback, which is known as the chattering-effect. This effect is caused when the control signal switches at a high frequency (see [7, 8]), causing several problems in the plant under control such as heat, mechanical wear, noise, and delay in the actuator response. The Twisting Algorithm (TA), is one of the main modalities of the so called High Order Sliding Mode Control (HOSM), which was designed to deal with the chattering-effect (see [9,10]). SMC is capable to modify the amplitude and the shape of the switching control signal by correctly tuning its parameters.

To achieve robustness with low levels of chattering, both the conventional SMC of the first order and the TA of the second order are chosen to set the basis of this work. Further, this study considers the use of proportional integral derivative (PID) control concepts to get adaptability and flexibility properties for the variable gains of the SM controller proposed along this manuscript. Even when traditionally, the SMC parameters are adjusted manually by trial and error, some previous efforts have been made in designing adaptive variable gains for the SMC, which constitutes the following state-of-the-art:

In [11], a robust adaptive SMC is proposed to deal with nonlinear systems with uncertain parameters. In [12] a logic concept is developed where the control gain depends on the distance of the system state to a discontinuity surface. In [13, 14], Lyapunov-based variable gains for the Super-Twisting algorithm are proposed to ensure the global and finite-time convergence to the desired sliding surface, claiming an attenuation of the chattering-effect; this approach is applied to linear time invariant systems. In [15] a new TA with dynamic adaptation gains is developed, in which the controller does not require complete information of system uncertainties. Regarding control of an electro-pneumatic actuator, in [16] an adaptive

Manuscript received May 9, 2019; revised August 23, 2019 and December 8, 2019; accepted January 5, 2020. Recommended by Associate Editor Guangdeng Zong under the direction of Editor Hamid Reza Karimi. This work was partially supported by the FORDECYT-CONACYT under grant 292399 of the National Council of Science and Technology in Mexico (CONACYT).

Sergio Alvarez-Rodríguez is with the Instituto Tecnológico José Mario Molina Pasquel y Henriquez, Lagos de Moreno, Jalisco 47480 México (e-mail: ser@cio.mx). Gerardo Flores is with the Centro de Investigaciones en Óptica, León, Guanajuato 37150, México (e-mail: gflores@cio.mx).
* Corresponding author.

Super-Twisting algorithm is proposed, where the Super-Twisting control gains are not overestimated. In [17] a nonlinear adaptive second order SM is presented to deal with system uncertainties and external disturbances. In [18], an Adaptive Continuous Twisting Algorithm is proposed, which produces a continuous control signal ensuring finite time convergence, this is due to the control signal compensates the Lipschitz perturbations in finite time. To achieve this goal the proposed controller needs the calculation of four different gains, this fact complicates the gain adjustment. In [19], a PID SMC is also proposed to reduce the chattering-effect, designed from the Lyapunov stability theory, for a specific class of uncertain nonlinear systems. In [20] an output feedback control law for the TA is designed to deal with uncertainties and disturbances, taking into account saturated control signals. In [21], an adaptive SMC framework is proposed for the tracking control of a particular class of uncertain nonlinear systems where the overall uncertainty of the system or its time derivative is not bounded by a constant. In [22], a PID sliding mode controller is proposed, which uses a multi-objetive optimization bat algorithm to control a gyroscope, however, this idea is focused only on the super-twisting (second order SMC). In [23], a robust adaptive controller is presented combining SMC with a kind of neural network to control industrial robot manipulators with uncertain dynamical environments. In [24], a SMC with variable gains is designed to not overestimate system disturbances, rejecting the chattering-effect by using the positioning tracking error, but, estimation of both future and past values of system states are not introduced yet. In [25], a sliding surface is designed from a conventional PID control according to system parameters, and the tuning rules for the PID are based on the assumption that the closed-loop poles are located in left hand side of the complex plane, nevertheless, this approach is focused only on SMC of the first order. In [26], a mass property-resilient controller for position and attitude control of a free-flying spacecraft is presented, which combines the two techniques, PID and SMC, however, this design has some troubles in dealing with the chattering-effect produced by the Sliding manifold. In [27], a combination between a self-tuning-fuzzy PID nonsingular-fast-termnal-sliding-mode control and a time delay estimator is proposed to control a PUMA robot, nevertheless, this approach becomes complex to implement on other applications. The most recent SM studies that hold on methodologies to deal with adverse effects caused by the uncertainties are presented in [28–30]. In [28], a SMC is applied to space robot manipulator models, under the assumption that these can be treated as nonlinear stochastic semi-Markovian switching systems. In [29], networked systems are considered to involve a Takagi-Sugeno model based SMC study. In the most recent [30], passivity-based robust SMC is involved to deal with a class of uncertain delayed system, using a state observer.

Even when the priority of the mentioned research works, is the application of adaptive principles or other novel strategies to increase the SM performance (e.g., to reduce the problems caused by the chattering-effect [31], increase the SM robust properties), the possibility to choose the order of the SMC, by just tuning the PID, has not previously proposed.

According to the state-of-the-art, the manuscripts that are most related to our work are [19, 22, 25–27]. In Table 1, a comparison of the main features and differences of these other control schemes with respect to our work, is presented.

Table 1. Comparison between the most recent PID SM control literature ([19, 22, 25–27]) and our research.

	[19]	[22]	[25]	[26]	[27]	Our Research
Is the proposed controller a multi-order approach?	No	No	No	No	No	Yes
Type of SMC involved	Conventional	Super-twisting	Conventional	Conventional	Conventional	First order and twisting
The level of chattering generated by the controller is:	Low	Low	Low-Medium	Medium-High	Low	Low
The robustness of the presented control system is:	High	High	High	High	High	High
The sensitivity to PID parameters of the controller is:	Low	Low-Medium	Medium	High	High	Low
Is it designed to deal with generic control systems?	Yes	No	No	No	No	Yes
The controller is designed to deal with:	Generic electro-mechanical systems	Gyroscope-type models	Levitation-based models	Space-craft based models	Exact dynamics math models	Generic electro-mechanical systems

1.1. Motivation

From the revision of the presented state-of-the-art and SM literature, three main drawbacks in implementing SMC can be mentioned:

1) Conventional SMC overestimates disturbances (even when the controller is correctly tuned). This drawback produces unnecessary amounts of chattering-effect.

2) Commonly, the controller is either of order one or of order two, i.e., the chance to select the controller's order by just tuning parameters does not exist in previous PID SM controllers.

3) Commonly, actuators constraints of the plant under control are not explicitly taken into account.

In the presented state-of-the-art and SM literature, issues 1 and 3, have been separately treated using different methods, but issue 2 has not been previously solved when PID principles are combined with SMC.

The motivation of this work, is to design a SM-based controller that simultaneously deal with these three issues, to obtain a control law with the potential to greatly simplify the task of robust control free from unnecessary chattering.

1.2. The main contribution

The main contribution of this work is the design of adaptive variable gains to obtain a SM-based controller, with the following properties:

The adaptive variable gains are adjusted taking the present, the past, and an estimation of future values of the tracking error magnitude. The resulting controller does not overestimates disturbances, but a minimum, necessary, and sufficient Sliding manifold is ensured, to maintain its robust properties.

The design allows to tune the controller as a first or as a second order SM controller (bi-order approach).

Actuators constraints are assumed bounded to obtain global exponential stability of the equilibrium point.

To achieve these SM control goals, the magnitude of the tracking error is used to feed proportional, integral, and derivative terms, for dynamic calculations of the adaptive variable gains, which are engaged from each other according to a novel design.

The main advantage of the proposed controller is the drastically reduction of the chattering-effect, saving energy consumption, but preserving the robust properties of SMC, when it is solving the trajectory tracking problem for the plant under control. Even when the controller does not overestimates internal and external disturbances, a rigorous stability analysis in the Lyapunov approach shows global exponential stability around the equilibrium point of the closed-loop control system.

The remainder of the document has the following presentation: in Section 2 the design of the proposed controller is presented; in Section 3, the stability analysis in the sense of Lyapunov is provided, as the proof of the given theorem; simulation results of controller performance are given in Section 4, where an inclined piston is the plant under control; a further discussion along with ideas for a future work is provided in Section 5; and finally, conclusions are presented in Section 6.

2. THE PROPOSED CONTROLLER

2.1. Problem setting

Consider the dynamical system,

$$\begin{aligned} \dot{x}_1 &= x_2, \\ \dot{x}_2 &= f(t) + u, \end{aligned} \tag{1}$$

where $x_1, x_2 \in \mathbb{R}$ are time dependant variables which represent the tracking and velocity errors respectively; $f(t) \in \mathbb{R}$ is a bounded function-possible dependent on the states which may include modelled and non-modelled dynamics of the plant, parametric variations, and disturbances; and $u \in \mathbb{R}$ represents the control variable. Variables $x_1(t), x_2(t)$ also construct the sliding manifold with the target

$$\begin{aligned} x_1 &= \chi_1 - x_d = 0, \\ x_2 &= \chi_2 - \dot{x}_d = 0, \end{aligned} \tag{2}$$

where χ_1, χ_2 represent the actual system states for position and velocity respectively, and $x_d(t) \in \mathbb{R}$ is the desired state of the plant (i.e., the reference signal to track).
The TA (see [9, 15, 33]), as a especial case of HOSM, has been designed for control systems with relative degree equals two, as such, system (1) can be controlled by

$$\begin{aligned} u &= -\mathrm{r}_1 \mathrm{sgn}(x_1) - \mathrm{r}_2 \mathrm{sgn}(x_2), \\ \mathrm{r}_1 &> \mathrm{r}_2 \geq 0, \end{aligned} \tag{3}$$

where $\mathrm{r}_1, \mathrm{r}_2 \in \mathbb{R}$ are the so called twisting parameters; and $\mathrm{sgn}(\cdot)$ is the well known sign function.

But system (1), can also be controlled by the conventional SMC of order one, which can be expressed as

$$u = -\mathrm{r}_1 \mathrm{sgn}(x_1), \tag{4}$$

for the case $r_2 = 0$.

The problem setting consist in extending the concept for r_1 and r_2 from constant parameters to Sliding and state-dependent variable gains,

$$\begin{aligned} \mathrm{r}_1 &\to \rho_1(x_1), \\ \mathrm{r}_2 &\to \rho_2(x_1). \end{aligned} \tag{5}$$

They are now called **SM adaptive variable gains**, rather than just constant gains.

These variable gains must adapt their values and the PID concept is proposed to achieve this goal.

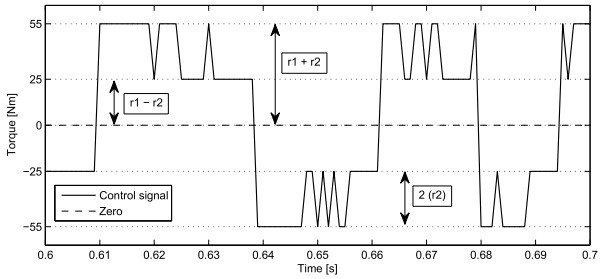

Fig. 1. Bounds of the control signal generated by the TA with $r_1 = 40$ and $r_2 = 15$.

2.2. Bounds of the SMC law of order two

According to (3), the bounds of the control (3) are

$$u = \begin{cases} r_1 + r_2, & \text{if : } \operatorname{sgn}(x_1) = \operatorname{sgn}(x_2) = -1, \\ -r_1 - r_2, & \text{if : } \operatorname{sgn}(x_1) = \operatorname{sgn}(x_2) = +1. \end{cases} \tag{6}$$

Note that the case $\operatorname{sgn}(x_1) \neq \operatorname{sgn}(x_2)$ ensures that the control signal is also bounded by $\max(|-r_1\operatorname{sgn}(x_1) - r_2\operatorname{sgn}(x_2)|)$ and $\min(-|-r_1\operatorname{sgn}(x_1) - r_2\operatorname{sgn}(x_2)|)$, where $|\cdot|$ represents the absolute value of any function. Also note that for the case $r_2 = 0$, (6) is also valid.

Fig. 1 is given to exemplify the region of the TA bounds given by (6), selecting $r_1 = 40$, $r_2 = 15$, and $U_0 = 55$ [Nm], where U_0 represents the saturation constraints of the plant or process to control, (e.g., the nominal limits of the actuators, and/or the operational limits of the plant). Also note that the TA parameters r_1 and r_2 must be selected, in such a way that the saturation constraints of the plant (U_0) cannot be exceeded, otherwise, the actuators could be damaged due to overloads with excessive amounts of power signals as electric currents, voltages, hydraulic flows, and so on. Thus, $r_1 + r_2 \leq U_0$ must be fulfilled.

2.3. Design of the proposed controller

Including (5) in (3),

$$\begin{aligned} &u = -\rho_1\operatorname{sgn}(x_1) - \rho_2\operatorname{sgn}(x_2), \\ &\rho_1 > \rho_2 \geq 0. \end{aligned} \tag{7}$$

Now, let us define the variable gains as

$$\begin{aligned} \rho_1 &= k_1\Gamma, \\ \rho_2 &= k_2\Gamma, \end{aligned} \tag{8}$$

where k_1, $k_2 \in \mathbb{R}^+$ are constant parameters, and $\Gamma = \Gamma(x_1, x_2)$ is a states dependant function. Giving rise to

$$u = -k_1\Gamma\operatorname{sgn}(x_1) - k_2\Gamma\operatorname{sgn}(x_2). \tag{9}$$

The next step is devoted to give the controller a bi-order feature [24].

To get a SMC of both first and second order (by just tuning parameters), a linear dependency between ρ_1 and ρ_2 is required. To achieve this goal, a parameter $\mu \in \mathbb{R}$ must be introduced, in the interval $0 \leq \mu < 1$, such that

$$\begin{aligned} k_1 &= \frac{1}{1+\mu}, \\ k_2 &= \mu k_1. \end{aligned} \tag{10}$$

Note that

$$k_1 + k_2 = \frac{1}{1+\mu} + \frac{\mu}{1+\mu} = 1. \tag{11}$$

Combining (8) with (11)

$$\Gamma(x_1, x_2) = \rho_1 + \rho_2, \tag{12}$$

which corresponds to the region for the bounds exemplified by (6) and Fig. 1. Note that $r_1 + r_2$ is a constant value, while $\rho_1 + \rho_2$ is a variable one in the interval $0 < \rho_1 + \rho_2 \leq U_0$.

Combining (8)-(12), control (7) is verified, and also the following linear dependency is obtained

$$\rho_2 = \mu\rho_1. \tag{13}$$

Observe that when $\mu = 0$, the SMC of order one is obtained as

$$u = -\Gamma\operatorname{sgn}(x_1). \tag{14}$$

As (12) just set the Γ bounds and does not provides the method to obtain its adaptive values, the final part of the controller design consists in propose the algorithm to obtain Γ using PID principles, as follows:

Let us include a proportional variable as $\Gamma_p(x_1)$, an integral term as $\Gamma_i(x_1)$, and a derivative one as $\Gamma_d(x_1, x_2)$. Each one of them are tracking error dependant functions. Now, define $\psi(x_1, x_2) = |\Gamma_p + \Gamma_i + \Gamma_d| \geq 0$, and, consider that $\Gamma = \Gamma(\psi)$.

Conventional PID control takes the tracking error to compute the control signal, however, in this study the absolute value for the tracking error is proposed to get the SM adaptive gains, otherwise the control system can be destabilized.

Let us introduce a constant gain γ_p, to give the controller **adaptability** and **flexibility**. The proportional term is proposed as

$$\Gamma_p = \gamma_p|x_1|, \tag{15}$$

where γ_p is a positive real number. Equation (15) takes into account the present values of the main sliding variable, however, its past and future values can also be considered.

The integral variable is designed as

$$\Gamma_i = \gamma_i \int_{t_0}^{t_1} |x_1| dt, \tag{16}$$

where γ_i is a positive real gain. Expression (16) accounts for past values of the sliding variable, then, if the output is not sufficient to reduce the size of x_1, the control variable will accumulate over time, causing the controller to apply a stronger action. Although the wind-up effect produced by PID control is not the subject of this work, it must be remembered that bounded integral gains must be appropriately selected to avoid saturation drawbacks.

The derivative variable is designed as

$$\Gamma_d = \gamma_d \frac{d}{dt}|x_1|, \tag{17}$$

where γ_d is also a positive real gain, and $\Gamma_d = \Gamma_d(x_1, x_2)$ because in the first time derivative of x_1, also x_2 explicitly appears. Equation (17) accounts for possible future values of the sliding variable, based on its current rate of change. In its expanded form ψ is given by,

$$\psi = \left| \gamma_p |x_1| + \gamma_i \int_{t_0}^{t_1} |x_1| dt + \gamma_d \frac{d}{dt}|x_1| \right|. \tag{18}$$

To tune $\gamma_p, \gamma_i, \gamma_d$, the Ziegler-Nichols technique, the algebraic method, or even the heuristic method can be used.

Even more, the case $\psi = 0$ is possible when $x_1 = x_2 = 0$ and when $\Gamma_p + \Gamma_i = |\Gamma_d|$ $\forall \Gamma_d < 0$, then, to ensure that the SM never decays to zero (i.e., the robust properties of the SMC remain $\forall t > 0$), a finite and positive constant $\delta \in \mathbb{R}$ is included in this design, in the interval $0 \leq \delta < U_0$, such that, the algorithm to dynamically update the value for Γ is proposed as

$$\Gamma(x_1, x_2) = \psi(x_1, x_2) + \delta. \tag{19}$$

Then, the adaptive variable gains are expressed in its expanded form as,

$$\begin{aligned} \rho_1 &= \left(\left| \gamma_p |x_1| + \gamma_i \int_{t_0}^{t_1} |x_1| dt + \gamma_d \frac{d}{dt}|x_1| \right| + \delta \right) k_1, \\ \rho_2 &= \left(\left| \gamma_p |x_1| + \gamma_i \int_{t_0}^{t_1} |x_1| dt + \gamma_d \frac{d}{dt}|x_1| \right| + \delta \right) k_2. \end{aligned} \tag{20}$$

In (20), $\rho_1 > \rho_2 \geq 0$ is fulfilled, because $k_1\Gamma > \mu(k_1\Gamma)$, for all $0 \leq \mu < 1$ and $\delta > 0$. Once again, it is easy to see that from (20) $\rho_1 + \rho_2 = \Gamma$, because $k_1 + k_2 = 1$.

As it can be seen ψ is designed as a non-negative function, to ensure that $\rho_1, \rho_2 \geq 0$, $\forall \delta, k_1 > 0$ and $k_2 \geq 0$. But remark that other way to obtain $\psi \geq 0$ is defining function (18) as $\psi = \Gamma_p + \Gamma_i + |\Gamma_d|$, however, when the three terms are positive $\forall t > 0$, the risk to get the well-known wind-up effect increases, while when allowing Γ_d to take also negative values, the system is less prone to saturation drawbacks.

Further, from the Adaptive Variable Gains of the Twisting Algorithm with PID (AVG-TA-PID) (9) and the Adaptive Variable Gains of the first order SM with PID (AVG-SM-PID) (14), both the conventional TA of order two and the conventional SMC of order one, can be obtained by making $\gamma_p = \gamma_i = \gamma_d = 0$, and selecting a convenient constant value for δ, thus, conventional SM controllers are included in the proposed control scheme.

Defining $\delta^* = 0$ to take the place of δ, $\Gamma = \psi$ is obtained. In such a case, the concept of "Sliding-PID" controller can be defined, which can be expressed similarly to (9) as

$$u = -k_1 \psi \text{sgn}(x_1) - k_2 \psi \text{sgn}(x_2). \tag{21}$$

From the concept of equation (21), also the Sliding-PI, and the Sliding-PD controllers can be suggested.

Remark 1: The amount and intensity of the chattering-effect produced by SMC depends on the amplitude and frequency of its switching control signal. The constant amplitude of the conventional second order SM (3) is $r_1 + r_2 = U_0$, while the variable amplitude of the control signal produced by (9) is given by $k_1\Gamma + k_2\Gamma = (k_1 + k_2)\Gamma = \Gamma$ (see (11)). Thus, the value of the amplitude of the proposed control only depends on Γ. As $\delta \leq \Gamma \leq U_0$, then $\Gamma \leq r_1 + r_2$. It is clear that the chattering produced by (9) never exceeds the one produced by (3), when both controllers work at the same frequency (theoretically infinite). Even more, in control (21) the chattering-effect decays to zero in the steady state (i.e., if $(x_1, x_2) = (0, 0)$, then $\psi = 0$, and the amplitude of the control action becomes zero).

In the real-world control implementations, overflows, overcharges, and other imbalances on the control signal may occur. To protect the control system from these drawbacks, and in order to not exceed actuator limits, the following assumption is presented:

Assumption 1: Control (9) is assumed bounded by $|u| \leq U_0$ where $U_0 \in \mathbb{R}^+$ is defined by the user considering actuator constraint (actuator's upper limit). Control (9), can also be expressed as

$$u = (\psi + \delta)[-k_1 \text{sgn}(x_1) - k_2 \text{sgn}(x_2)].$$

According to the natural behaviour of the SMC of order two (see Fig. 1), the bounds of the control signal are reached only when $\text{sgn}(x_1) = \text{sgn}(x_2) = \pm 1$. Then, for the upper and lower variable bounds, $|u| = (\psi + \delta)[k_1 + k_2]$. Involving (11), it is obtained $\psi = |u| - \delta$ (which is also valid for the SMC or order one). Then, the following inequality holds

$$\psi \leq U_0 - \delta = \rho, \tag{22}$$

where $\rho \in \mathbb{R}_0^+$.

3. STABILITY ANALYSIS

In this section global exponential stability of the closed-loop system is demonstrated via Lyapunov analysis. The following theorem resumes the main result of this paper.

Theorem 1: Consider the nonlinear system (1) and Assumption 1, then the control law

$$u = -k_1\Gamma(x_1,x_2)\,\mathrm{sgn}(x_1) - k_2\Gamma(x_1,x_2)\,\mathrm{sgn}(x_2),$$

where

$$\Gamma = \underbrace{\left|\gamma_p|x_1| + \gamma_i\int_{t_0}^{t_1}|x_1|dt + \gamma_d\frac{d}{dt}|x_1|\right|}_{\psi(x_1,x_2)\le\rho} + \delta,$$

with $\gamma_p,\ \gamma_i,\ \gamma_d,\ \delta \in \mathbb{R}^+$,

globally exponentially stabilizes the origin of (1)-(2).

Proof: The proof is divided in two parts. The first part demonstrates that the closed-loop trajectories are bounded. The second part finish the proof using the first results obtaining a global exponential stability.

Consider the following candidate Lyapunov function, inspired by [34]

$$V(x_1,x_2) = \bar{a}|x_1| + \frac{1}{2}x_2^2. \tag{23}$$

where $\bar{a} \in \mathbb{R}$ is a positive definite constant.

As $\frac{d}{dt}|x_1| = \dot{x}_1\mathrm{sgn}(x_1)$, $\frac{d}{dt}x_2^2 = 2x_2\dot{x}_2$, $\dot{x}_1 = x_2$ and $\dot{x}_2 = f(t)+u$ (as stated in (1)), the time-derivative of (23) is computed as follows:

$$\dot{V} = \bar{a}x_2\mathrm{sgn}(x_1) + x_2\left(f(t)+u\right). \tag{24}$$

Substituting the control (9) in (24) it follows that

$$\begin{aligned}\dot{V} =& \bar{a}x_2\mathrm{sgn}(x_1) + x_2f(t) - k_1\Gamma(x_1,x_2)x_2\mathrm{sgn}(x_1)\\ &- k_2\Gamma(x_1,x_2)x_2\mathrm{sgn}(x_2).\end{aligned} \tag{25}$$

Substituting (19) in (25),

$$\begin{aligned}\dot{V} =& \bar{a}x_2\mathrm{sgn}(x_1) + x_2f(t) - k_1\psi(x_1,x_2)x_2\mathrm{sgn}(x_1)\\ &- k_1\delta x_2\mathrm{sgn}(x_1) - k_2\Gamma(x_1,x_2)|x_2|,\end{aligned}$$

then, if $\bar{a} = k_1\delta$ and considering the boundedness of $f(t)$, i.e. $|f(t)| \le c$ it follows that

$$\begin{aligned}\dot{V} \le& -k_1\psi(x_1,x_2)x_2\mathrm{sgn}(x_1) - k_2\Gamma(x_1,x_2)|x_2| + c|x_2|\\ \le& k_1|\psi(x_1,x_2)||x_2| - k_2\psi(x_1,x_2)|x_2| - k_2\delta|x_2| + c|x_2|,\end{aligned}$$

where we have used (19). Then,

$$\dot{V} \le (k_1-k_2)\,|\psi(x_1,x_2)||x_2| - (k_2\delta - c)\,|x_2|.$$

In the last inequality we consider that $k_1 > k_2$ to accomplish the well-known restriction in the second order sliding mode based-control. Then $(k_1-k_2) = r > 0$ and using Assumption 1 for this part of the proof we conclude that

$$\begin{aligned}\dot{V} \le& -(k_2\delta - c - r|\psi(x_1,x_2)|)\,|x_2|\\ \le& -(k_2\delta - c - r\rho)\,|x_2| \le 0,\end{aligned} \tag{26}$$

as long as

$$k_2 > \frac{c+r\rho}{\delta} = \frac{c+r(U_0-\delta)}{\delta}.$$

Last inequality shows that the closed-loop system is stable and the closed-loop trajectories are bounded.

In order to demonstrate that the closed-loop system is GES let consider the following second part of this analysis. Define the compact set

$$\Omega_l = \{(x_1,x_2) \in \mathbb{R}^2, V(x_1,x_2) \le l\}, \tag{27}$$

where $V \in \mathbb{R}^+$ and Ω_l is an arbitrarily small vicinity with centre at the origin. Let's propose a positive definite function $V_\Omega > 0 \setminus \{(x_1,x_2) = 0\}$ in Ω_l, given as

$$V_\Omega = V + V_1 = \underbrace{\bar{a}|x_1| + \frac{1}{2}x_2^2}_{V} + \underbrace{Kx_1x_2}_{V_1}, \tag{28}$$

where the function $V_1 = Kx_1x_2$ with $K \in \mathbb{R}^+$ has been added to the original Lyapunov function V. From the compact set Ω_l in (27) and (28) it follows that

$$|x_1| \le \frac{l}{\bar{a}} \text{ and } |x_2| \le \sqrt{2l}. \tag{29}$$

To observe the positive definiteness of V_Ω consider that the polynomial $K(x_1+x_2)^2$ is positive for all (x_1,x_2) except when $x_1 = x_2 = 0$.
Then $K(x_1+x_2)^2 = K\left(x_1^2 + 2x_1x_2 + x_2^2\right) > 0$, and thus

$$Kx_1x_2 \ge -\frac{K}{2}x_1^2 - \frac{K}{2}x_2^2.$$

Combining (28) and (29) it follows that

$$\begin{aligned}V_\Omega =& \bar{a}|x_1| + \frac{1}{2}x_2^2 + Kx_1x_2\\ \ge& \bar{a}|x_1| + \frac{1}{2}x_2^2 - \frac{K}{2}x_1^2 - \frac{K}{2}x_2^2\\ \ge& \frac{1}{2}(1-K)x_2^2 + \left(\bar{a} - \frac{lK}{2\bar{a}}\right)|x_1| > 0,\end{aligned} \tag{30}$$

with $K = \min\{1, \frac{2\bar{a}^2}{l}\}$ in Ω_l except at the origin $(x_1,x_2) = (0,0)$.

Now lets compute the time derivative of $V_1 = Kx_1x_2$,

$$\begin{aligned}\dot{V}_1 =& Kx_2^2 + K(x_1)\left(f(t) - k_1\Gamma(x_1,x_2)\mathrm{sgn}(x_1)\right.\\ &\left. - k_2\Gamma(x_1,x_2)\mathrm{sgn}(x_2)\right)\\ \le& Kx_2^2 + Kc|x_1| - Kk_1\Gamma(x_1,x_2)|x_1|\\ &+ Kk_2\Gamma(x_1,x_2)|x_1|.\end{aligned}$$

The last inequality holds because $\Gamma(\cdot) = |\Gamma(\cdot)|$. Since $\Gamma = \psi + \delta$,

$$\begin{aligned}\dot{V}_1 \le& K(x_2^2 + c|x_1| - k_1\psi(x_1,x_2)|x_1|\\ &- k_1\delta|x_1| + k_2\psi(x_1,x_2)|x_1| + k_2\delta|x_1|).\end{aligned}$$

We know that $0 \leq \psi \leq \rho$ and from the first part of the proof also $k_1 > k_2$, then,

$$\dot{V}_1 \leq K(x_2^2 + c|x_1| - k_1\delta|x_1| + k_2\delta|x_1|), \text{ or}$$
$$\dot{V}_1 \leq K(|x_2||x_2| - (k_1\delta - k_2\delta - c)|x_1|).$$

From the last inequality and (26) the time derivative of V_Ω is given by

$$\begin{aligned}\dot{V}_\Omega \leq & -(k_2\delta - c - r\rho)|x_2| + K|x_2||x_2| \\ & -(Kk_1\delta - Kk_2\delta - Kc)|x_1| \\ \leq & -\left(k_2\delta - c - r\rho - K\sqrt{2l}\right)|x_2| \\ & -(Kk_1\delta - Kk_2\delta - Kc)|x_1|, \end{aligned} \tag{31}$$

since $|x_2| \leq \sqrt{2l}$ in the compact set Ω_l. And $\dot{V}_\Omega \leq 0$ holds provided that

$$\begin{aligned} & k_1 > k_2 + \frac{c}{\delta}, \\ & k_2 > \frac{c + r\rho + K\sqrt{2l}}{\delta}, \end{aligned} \tag{32}$$

from which $k_1 > k_2 > 0$. Remark that for an extremely perturbed system, i.e., $c >> r, \rho, K, l$, (32) become

$$\begin{aligned} & \delta k_1 > 2c, \\ & \delta k_2 > c, \text{or} \\ & k_1 > 2k_2. \end{aligned} \tag{33}$$

Furthermore from (31) we conclude that

$$\begin{aligned}\dot{V}_\Omega \leq & -|x_2|\left(k_2\delta - c - r\rho - K\sqrt{2l}\right) \\ & -|x_1|K(k_1\delta - k_2\delta - c) \\ \leq & -\gamma(|x_1| + |x_2|), \end{aligned} \tag{34}$$

where $\gamma = \min\{k_2\delta - c - r\rho - K\sqrt{2l}, K(k_1\delta - k_2\delta - c)\}$. Notice that the compact set (27) can be arbitrarily large; this achieves a global result. □

4. SIMULATION RESULTS

4.1. Stability result

Fig. 2 shows a simulation of the actual behaviour of $\dot{V}$ for the closed-loop control system (1), perturbed with a white noise function (in thick line), which is bounded by an amplitude from +5.5 to −5.5 and a frequency of ∼ 26.67 [Hz]. It can be observed that $\dot{V}$ (in thin line) has always values under the zero, and the simulation confirms stability for the closed-loop system.

4.2. Implementation example

The system under consideration to obtain simulation results is an inclined piston, with the following dynamics,

$$\dot{x}_1 = x_2,$$

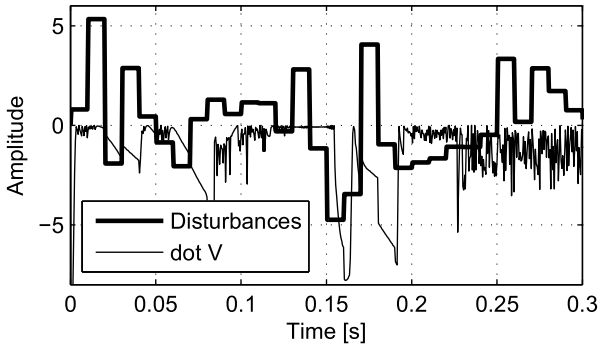

Fig. 2. Behaviour of $\dot{V}$ for the perturbed system.

$$\dot{x}_2 = -I^{-1}[f_{friction} + f_{noise} + f_{grav}] + I^{-1}u, \tag{35}$$

where I is the inertia moment and has the value $I = 1$; the friction force is $f_{friction} = 0.14 + 0.27\text{sgn}(x_2)$; f_{noise} is a random white noise function bounded by an amplitude of 2.3 [Nm], and frequency of ∼ 650 [Hz]; the gravitational force is $f_{grav} = 4.12$ [N]; and u represents the control law (9), which is bounded by the actuator constraint $U_0 = 75$ [Nm].

Simulations taking the AVG-TA-PID were preferred, because the AVG-SM-PID of the first order is included in the first one. The AVG-TA-PID has been tuned with the intermediate value $\mu = 0.5$ (except for Fig. 3). The lower bound for the SM has been selected as $\delta = U_0/3 = 25$ [Nm] (except for Fig. 6), while $\gamma_p = 1000$, $\gamma_i = 100$, and $\gamma_d = 100$. The reference signal to track was selected as a square wave form with an amplitude of 0.4 [m] (from -0.2 to 0.2), with frequency of 0.5 [Hz].

4.2.1 Study of μ and δ

The way to select γ_p, γ_i and γ_d is widely studied in literature relate to PID tuning, however, about the way to select μ and δ there is not any information (since they belong to novel control designs). Thus, from simulation results, the behaviour of the controller working under different values of μ and δ is studied, and mathematical tools are proposed to help the designer in understanding its behaviour to select them according to specific applications.

Fig. 3 shows a generic behaviour of AVG-TA-PID controller tracking the specified reference signal located at 0.2 [m], with values of μ selected from 0 to 0.6, (this is the range that showed better robustness performance in simulations for the perturbed system (35)). As it can be observed, the higher the value of μ, the more the convergence time increases, and, the value of the corresponding overshoot peak decreases. Thus, the inverse of the amplitude value of overshoots can be considered as an index of convergence time, according to the model

$$t_C = \alpha\frac{1}{\eta}, \tag{36}$$

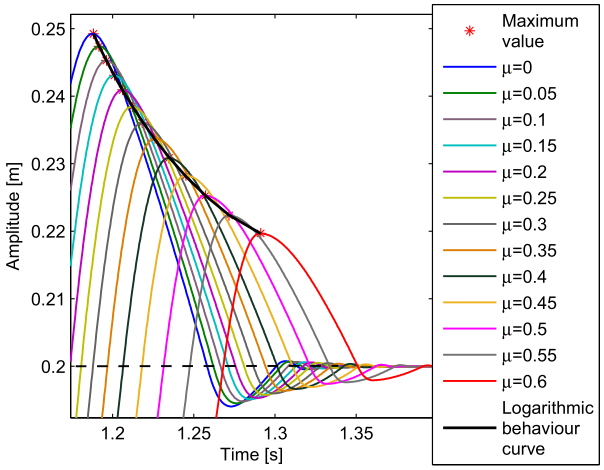

Fig. 3. Behaviour of the AVG-TA-PID controller working with different values of μ (from 0 to 0.6) and $\delta = 25$.

where, t_C is the convergence time, η is the maximum overshoot amplitude, and $\alpha > 0$ is a correlation function. Taking the maximum value in each overshoot peak to measure its amplitude, a natural decay process can be observed (see the logarithmic behaviour curve in Fig. 3), which can be modelled by the differential decay equation

$$\dot{\eta} = \beta\eta, \eta(t_0) = \max(\eta), \tag{37}$$

where $\beta > 0$ is a constant gain, and t_0 is initial time. As it is well known, the general solution of (37) is

$$\eta(t) = Ce^{\beta t_P}, \tag{38}$$

where C is a constant of integration, and t_P is the time to get the maximum overshoot value.

Note that two initial conditions are needed to get particular solutions from (38), and the statistical α is required to estimate t_C from (36), for every desired value of μ.

For the application example under consideration, two initial conditions measured in the logarithmic curve are $\eta(1.1967) = 0.2453$ and $\eta(1.2343) = 0.2308$, for $\mu = 0.1$ and $\mu = 0.4$ respectively. Substituting this data in (38), the following particular solution is obtained

$$\eta = 1.7057e^{-1.6205t_P}. \tag{39}$$

Even more, when more than two initial conditions are available, graphics of time versus μ can be obtained, as those given in Fig. 4, where actual values of time of the overshoot peak are represented in the left hand side (dashed blue curve), while actual values of convergence time are in the right hand side (dashed cyan curve). Both curves can be easily adjusted by polynomial expressions of the form

$$y = a_n x^n + \cdots + a_2 x^2 + a_1 x + a_0. \tag{40}$$

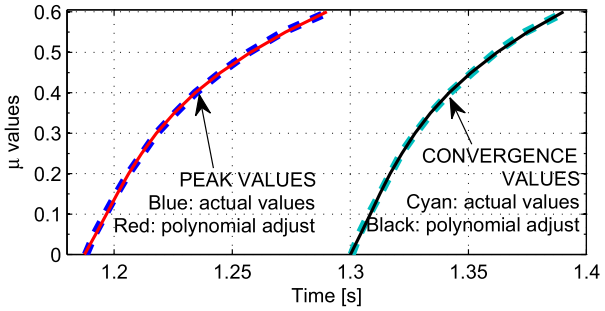

Fig. 4. The t_P (left side curves) and t_C (right side curves) versus μ values, along with their polynomial adjusts.

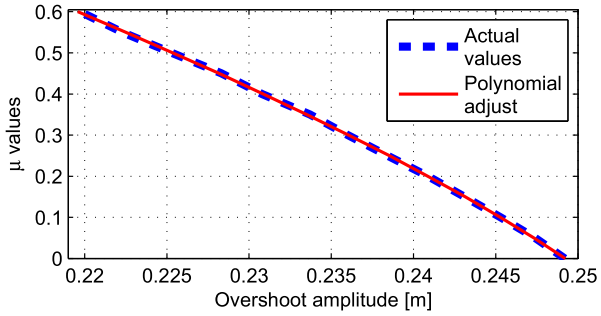

Fig. 5. Overshoot amplitude versus μ values, along with its respective polynomial adjust.

For our example, $n = 3$ (which is more than enough), and according to data obtained from simulations, the polynomials are

$$\begin{aligned} t_P &= 0.3746\mu^3 - 0.1056\mu^2 + 0.0996\mu + 1.1874, \\ t_C &= 0.3182\mu^3 - 0.0886\mu^2 + 0.0889\mu + 1.3001, \end{aligned} \tag{41}$$

which are the red and black curves respectively in Fig. 4. Graphic η versus μ is given in Fig. 5, where actual values are represented in dashed blue line, and its polynomial adjust is

$$\eta = 0.0079\mu^3 - 0.0254\mu^2 - 0.037\mu + 0.2492. \tag{42}$$

Using (41)-(42), the time to reach the peak, the convergence time, and the maximum overshoot amplitude, can be estimated for any value of μ, and also an estimation for α in (36) can be obtained.

Numerical example: Let us consider $\mu = 0.35$, then, according to (41), $t_P = 1.2254$ s and $t_C = 1.334$ s, while according to (42), $\eta = 0.2335$. These results are in accordance to (39).

Further, observe in Fig. 6, that the behaviour of the controller for different values of δ (fixing μ at any desired

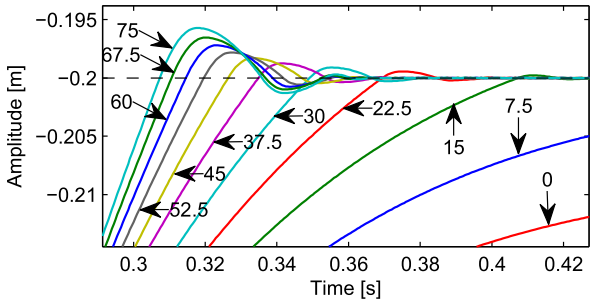

Fig. 6. Behaviour of the AVG-TA-PID controller working with different values of δ (from 0 to $U_0 = 75$) and $\mu = 0.5$.

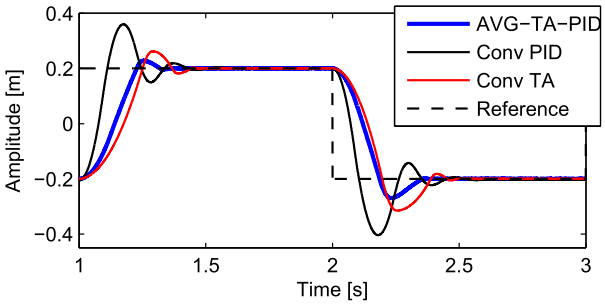

Fig. 7. Tracking process for AVG-TA-PID, Conventional PID, and Conventional TA.

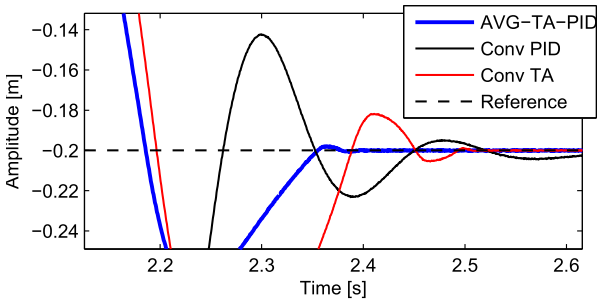

Fig. 8. Zoom view to show convergence time for the three controllers.

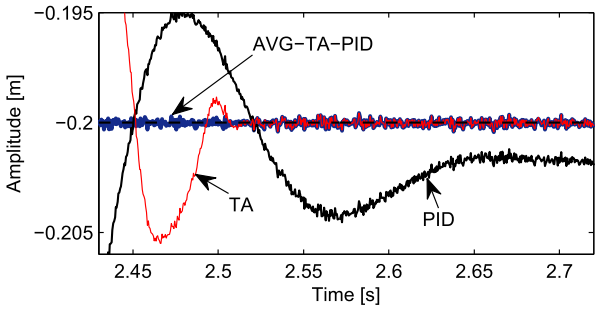

Fig. 9. Fail of PID in tracking the reference signal.

value), has also a similar logarithmic behaviour. Thus, the same method can be used to estimate t_P, t_C, and η for any value of parameter δ. According to this methodology, accurate estimations for the convergence time and features of the overshoot can be obtained for every value of μ and/or δ, to help the reader in selecting parameters according to every specific application and needing.

4.2.2 Performance results

Results to know the actual performance of the AVG-TA-PID controller compared with the TA and PID controllers are showing up next.

After a large number of simulations, the best parameters for TA and PID controllers were heuristically obtained, to simultaneously get a correct combination of robustness, fast convergence, and low chattering levels, for the control of (35). They are: $r_1 = 46$, and $r_2 = 29$ for the conventional TA; and $K_p = 1052$, $K_i = 348$, and $K_d = 21$ are the classic PID gains for the proportional, integral and derivative terms, respectively.

Taking these working conditions, Fig. 7 shows the comparative performance for AVG-TA-PID (thick line), conventional PID (dashed line), and the conventional TA (thin line). As it can be seen, the AVG-TA-PID the lower overshoot in the transient.

Fig. 8 is an enlarged view of Fig. 7 to show the convergence time for the three controllers, where it is clear that AVG-TA-PID has the faster convergence. Fig. 9 is a zoom view inside Fig. 8, to show that the PID controller is unable to satisfactory reach convergence under the presence of the gravitational force.

It is worth to mention that the apparent discontinuities appearing in the PID line, are just produced by the white noise function specified in system (35), since according to theory, PID is free from chattering, although without the robust properties of SMC. When the PID is tuned to reduce the overshoot ($K_p = 150$, $K_i = 115$ and $K_d = 25$), a similar overshoot to the AVG-TA-PID is obtained, however, for this case, convergence is not achieved to the proposed reference signal, for the dynamics of the plant under control, as it can be observed in Fig. 10. Even more, increasing values for K_i also increases the risk to get the wind-up effect. Fig. 11 shows the control signals produced by conventional PID, conventional TA, and the AVG-TA-PID controllers, where it can be seen the nature of both continuous and discontinuous control signals. As it can be observed the PID (in black thick line) is saturated at $+75$ and -75 [Nm] in the transient by the actuators constraints (avoiding large overshoots), and before it arrives to the steady state (0.35 s approximately), it becomes a continuous signal. Conventional TA (in red line) and the AVG-TA-PID (in blue line) present discontinuous control signals once the steady state is achieved, but observe that the

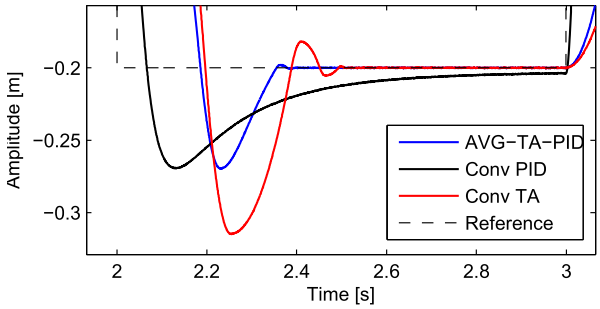

Fig. 10. Low overshoot of PID in tracking the reference signal.

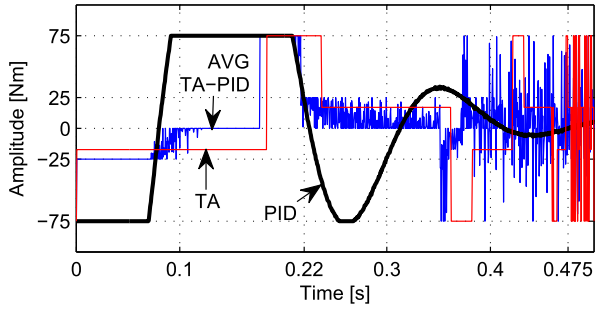

Fig. 11. Control signal produced by AVG-TA-PID, PID, and Twisting controllers.

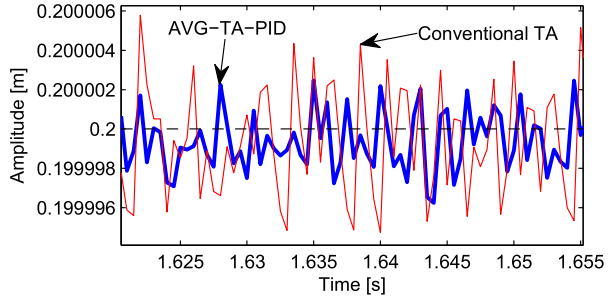

Fig. 12. Chattering-effect produced by controllers under study.

AVG-TA-PID reaches the steady faster than the conventional TA, i.e., the sliding manifold for the AVG-TA-PID is performed at 0.22 s (even at the nearest of 0.1 s there is a small manifold), while the conventional TA reaches its characteristic discontinuous control at 0.475 s. It is important to remember that according to theory [9], high frequency discontinuous control provides robust properties around the system's equilibrium point, as such, Fig. 11 also shows that both AVG-TA-PID and conventional TA present much more robustness respect the PID control. Fig. 12 shows the actual vibration resulting from the combination of the control signals produced by the SM (shown in Fig. 11) and the dynamics of the plant. For AVG-TA-PID (thick line) vs the conventional TA (thin line). As it can be observed, the frequency for both is nearly the same (∼700 [Hz]), however, the amplitude for the TA is 0.000012 [m], while for the AVG-TA-PID is 0.0000055 [m]. Thus, the chattering-effect for the TA is twice than that of the AVG-TA-PID, under the specified working conditions. It is important to note that in this figure the line for the PID is out of the graphic because it do not achieved convergence.

5. FURTHER DISCUSSION

For the case in which $|x_1(0)| >> |x_d|$, $|x_2(0)| >> |\dot{x}_d|$, the tracking errors (for position and velocity) have large values, such that Γ has automatically the maximum possible value, while when the tracking errors are both zero, the response for the controller must be the minimum, necessary, but sufficient to maintain the convergence attached to the reference signal. Thus, for nonautonomous systems,

$$\begin{aligned}&\Gamma(x_1,x_2,0) = U_0,\\ &\Gamma(0,0,t) = \delta.\end{aligned} \tag{43}$$

Another conclusion which can lead to future works, is that taking the referenced nominal Sliding system

$$x_2 = f(x_1,x_2,t) \tag{44}$$

and considering that f, $g : [0,\infty) \times D \to \mathbb{R}^n$ are piecewise continuous in t and locally Lipschitz in x_1 on $[0,\infty) \times D$, and $D \to \mathbb{R}^n$ is a domain which contains the origin $(0,0)$, then for the perturbed nonautonomous system

$$x_2 = f(x_1,x_2,t) + g(x_1,x_2,t), \tag{45}$$

(19) can be expressed by the most general form

$$\Gamma = \gamma_p x_1 + \gamma_i \int_{t_0}^{t_1} x_1, dt + \gamma_d \frac{d}{dt} x_1 + g(x_1,x_2,t)w, \tag{46}$$

were w is a secondary control variable, and $g(x_1,x_2,t)w$ is the control term designed specifically to predict and reject perturbations and noise.

6. CONCLUSIONS

A technique to obtain adaptive variable gains, using PID principles, has been designed for the SMC, which can be tuned as a controller of order one, or order two (bi-order approach). This is a robust SM-based controller capable to reject unnecessary chattering, since it does not overestimate external perturbations, noise, and non-modelled dynamics. The stability analysis shows Global Exponential Stability in the sense of Lyapunov, for the trajectories of

the control system under the action of the proposed control technique.

Simulation results obtained from an electromechanical system, show that the novel control technique has better performance (in solving the trajectory tracking problem) than both the conventional TA and the classical PID controllers. In the same way, the AVG-TA-PID controller significantly reduces the chattering-effect with respect to the conventional TA.

Even more, the design of AVG-TA-PID helps in saving energy, because it does not overestimate disturbances by switching off unnecessary power control actions, as such, this is an environmentally friendly controller.

REFERENCES

[1] B. Bandyopadhyay, S. Janardhanan, and S. Spurgeon, *Advances in Sliding Mode Control: Concept, Theory and Implementation*, Springer-Verlag, Berlin Heidelberg, 2013.

[2] Y. Fang and T. Chow, "Chattering free sliding mode control based on recurrent neural network," *Proc. of IEEE International Conference on Systems, Man, and Cybernetics*, San Diego, October 1998.

[3] K. Jezernik, "Robust chattering-free sliding mode control of servo drives," *International Journal of Electronics*, vol. 80, no. 2, pp. 169-179, February 1996.

[4] L. Fridman, "An averaging approach to chattering," *IEEE Transactions on Automatic Control*, vol. 46, no. 8, pp. 1260-1265, August 2001.

[5] A. Levant, "Chattering analysis," *IEEE Transactions on Automatic Control*, vol. 55, no. 6, pp. 1380-1389, February 2010.

[6] L. Fridman, J. Moreno, and R. Iriarte, *Sliding Modes after the First Decade of the 21st Century: State of the Art*, Springer-Verlag, Berlin Heidelbert, 2011.

[7] G. Bartolini, "Chattering phenomena in discontinuous control systems," *Int. J. Systems Sci.*, vol. 20, no. 12, pp. 2471-2481, December 1989.

[8] I. Boiko and L. Fridman, "Analysis of chattering in continuous sliding-mode controllers," *IEEE Transactions on Automatic Control*, vol. 50, no. 9, pp. 1442-1446, September 2005.

[9] A. Levant, "Sliding order and sliding accuracy in sliding mode control," *International Journal of Control*, vol. 58, no. 6, pp. 1247-1263, December 1993.

[10] L. Dorel and A. Levant, "On chattering-free," *Proceedings of the 47th IEEE Conference on Decision and Control*, Cancún, México, pp. 2196-2201, December 2008.

[11] Y.-J. Huang, T.-C. Kuo, and S.-H. Chang, "Adaptive sliding-mode control for nonlinear systems with uncertain parameters," *IEEE Transactions on Systems, Man, and Cybernetics, Part B: Cybernetics*, vol. 38, no. 2, pp. 534-539, April 2008.

[12] F. Plestan, Y. Shtessel, V. Brégeault, and A. Poznyak, "New methodologies for adaptive sliding mode control," *International Journal of Control*, vol. 83, no. 9, pp. 1907-1919, June 2010.

[13] T. González, J. Moreno, and L. Fridman, "Variable and adaptive gain super-twisting sliding mode control," *IEEE Transactions on Automatic Control*, vol. 57, no. 8, pp. 2100-2105, August 2012.

[14] E. Cruz-Zavala, J. Moreno, and L. Fridman, "Adaptive gains super-twisting algorithm for systems with growing perturbations," *Proc. of the 18th IFAC World Congress*, Milano, pp. 3039-3044, January 2011.

[15] M. Taleb, A. Levant, and F. Plestan, "Twisting algorithm adaptation for control of electropneumatic actuators," *Proc. of IEEE International Workshop on Variable Structure Systems (VSS)*, Mumbai, pp. 178-183, January 2012.

[16] Y. Shtessel, M. Taleb, and F. Plestan, "A novel adaptive-gain supertwisting sliding mode controller: Methodology and application," *Automatica*, vol. 48, no. 5, pp. 759-769, May 2012.

[17] L. Yu, M. Zhang, and Z. Fei, "Nonlinear adaptive sliding mode switching control with average dwell-time," *International Journal of System Science*, vol. 44, no. 3, pp. 471-478, March 2013.

[18] J. Moreno, Y. Negrete, V. Torres-González, and L. Fridman, "Adaptive continuous twisting algorithm," *International Journal of Control*, vol. 89, no. 9, pp. 1798-1806, September 2016.

[19] S. Mobayen, "An adaptive chattering-free PID sliding mode control based on dynamic sliding manifolds for a class of uncertain nonlinear systems," *Nonlinear Dynamics*, vol. 82, no. 1-2, pp. 53-60, October 2015

[20] M. A. Golkani, L. Fridman, S. Koch, M. Reichhartinger, and M. Horn, "Observer-output saturated output feedback control using twisting algorithm," *Proc. of 14th International Workshop on Variable Structure Systems (VSS)*, Nanjing, China, June 2016.

[21] S. Roy, S. B. Roy, and I. N. Kar, "A new design methodology of adaptive sliding mode control for a class of nonlinear systems with state dependent uncertainty bound," *Proc. of 15th International Workshop on Variable Structure Systems*, Austria, July 2018.

[22] M. Rahmani, H. Komijani, A. Ghanbari, and M. M. Ettefagh, "Optimal novel super-twisting PID sliding mode control of a MEMS gyroscope based on multi-objective bat algorithm," *Microsystem Technologies*, vol. 24, no. 6, pp. 2835-2846, June 2018.

[23] V. T. Yen, W. Y. Nan, and P. V. Cuong, "Robust adaptive sliding mode neural networks control for industrial robot manipulators," *International Journal of Control, Automation and Systems*, vol. 17, no. 3, pp. 783-792, March 2019.

[24] S. Alvarez-Rodríguez, G. Flores, and N. Alcalá Ochoa, "Variable gains sliding mode control," *International Journal of Control, Automation and Systems*, vol. 17, No. 3, pp. 555-564, March 2019.

[25] A. V. Starbino and S. Sathiyavathi, "Real-time implementation of SMC-PID for magnetic levitation system," *Sādhanā*, vol. 44, no. 115, pp. 1-13, May 2019.

[26] H. Hettrick and J. Todd, "In-flight adaptive PID sliding mode position and attitude controller," *Proc. of IEEE Aerospace Conference*, pp. 1-9, Big Sky, MT, USA, March 2019.

[27] M. Van, X. P. Do, and M. Mavrovouniotis, "Self-tuning fuzzy PID-nonsingular fast terminal sliding mode control for robust fault tolerant control of robot manipulators," *ISA Transactions*, 2019. DOI: 10.1016/j.isatra.2019.06.017

[28] W. Qi, G. Zong, and H. R. Karimi, "Sliding mode control for nonlinear stochastic semi-Markov switching systems with application to space robot manipulator model," *IEEE Transactions on Industrial Electronics*, vol. 67, no. 5, pp. 3955-3966, 2020.

[29] B. Jiang, H. R. Karimi, Y. Kao, and C. Gao, "Takagi-Sugeno model based event-triggered fuzzy sliding mode control of networked control systems with semi-Markovian switchings," *IEEE Transactions on Fuzzy Systems*, 2019. DOI: 10.1109/TFUZZ.2019.2914005

[30] Z. Liu, H. R. Karimi, and J. Yu, "Passivity-based robust sliding mode synthesis for uncertain delayed stochastic systems via state observer," *Automatica*, vol. 111, 2020.

[31] V. Utkin and A. Pozniak, "Adaptive sliding mode control with application to super-twisting algorithm: Equivalent control method," *Automatica*, vol. 49, no. 1, pp. 39-47, January 2013.

[32] V. Utkin, J. Guldner, and J. Shi, *Sliding Mode Control in Electromechanical Systems*, CRC Press, New York, 1999.

[33] Y. Dvir and A. Levant, "Accelerated twisting algorithm," *IEEE Transactions on Automatic Control*, vol. 60, no. 10, pp. 2803-2807, October 2015.

[34] Y. Orlov, "Finite time stability and robust control synthesis of uncertain switched systems," *SIAM J. Control Optim.*, vol. 43, no. 4, pp. 1253-1271, July 2006.

Sergio Alvarez-Rodríguez received his post-graduated degree in mechatronics engineering from Centro Nacional de Investigación y Desarrollo Tecnológico, México, in 2007. He received a Ph.D. degree in Science and Technology from Universidad de Guadalajara, México, in 2014, and from February 2016 to July 2017 he made a post-doctoral stay at Optical Research Center, AC. He is currenlty a full time researcher professor at TecMM, Lagos de Moreno, Jalisco, México. His areas of interest are on robotics, control theory, and sensors for instrumentation.

Gerardo Flores received his B.S. degree in Electronic Engineering with honors from the Instituto Tecnológico de Saltillo, México in 2000; an M.S. degree in Automatic Control from CINVESTAV-IPN, Mexico City, in 2010; and a Ph.D. degree in Systems and Information Technology from the Heudiasyc Laboratory of the Université de Technologie de Compiègne - Sorbonne Universités, France in October 2014. Since August 2016, he has been a full time researcher and the head of the Perception and Robotics LAB with the Center for Research in Optics, León Guanajuato, Mexico. His research interests are focused on the theoretical and practical problems arising from the development of autonomous robotic systems and vision systems. Dr. Flores has published more than 40 papers in the areas of control systems, computer vision and robotics.